Osteoarthritis and Cartilage 29 (2021) 1720–1731

Osteoarthritis and Cartilage

OARSI OSTEOARTHRITIS RESEARCH SOCIETY INTERNATIONAL

Cannabinoid receptor type 2 is upregulated in synovium following joint injury and mediates anti-inflammatory effects in synovial fibroblasts and macrophages

P. Rzeczycki, C. Rasner, L. Lammlin, L. Junginger, S. Goldman, R. Bergman, S. Redding, A.J. Knights, M. Elliott, T. Maerz*

Orthopaedic Research Laboratories, Department of Orthopaedic Surgery, University of Michigan, Ann Arbor, MI, USA

ARTICLE INFO

Article history:
Received 11 January 2021
Accepted 6 September 2021

Keywords:
Post-traumatic osteoarthritis
Endocannabinoid system
Macrophage
Nociception
Synovitis

SUMMARY

Objective: Joint injury-induced perturbations to the endocannabinoid system (ECS), a regulator of both inflammation and nociception, remain largely uncharacterized. We employed a mouse model of ACL rupture to assess alterations to nociception, inflammation, and the ECS while using *in vitro* models to determine whether CB2 agonism can mitigate inflammatory signaling in macrophages and fibroblast-like synoviocytes (FLS).

Design: Mice underwent noninvasive ACL rupture (ACLR) via tibial compression-based loading. Nociception was measured longitudinally using mechanical allodynia and knee hyperalgesia testing. Synovitis was assessed using histological scoring and histomorphometry. Gene and protein markers of inflammation were characterized in whole joints and synovium. Immunohistochemistry assessed injury-induced alterations to CB1+, CB2+, and F4/80+ cells in synovium. To assess whether CB2 agonism can inhibit pro-inflammatory macrophage polarization, murine bone marrow-derived macrophages (mBMDM) were stimulated with IL-1β or conditioned medium from IL-1β-treated FLS and treated with vehicle (DMSO), the CB2 agonist HU308, or cannabidiol (CBD). Macrophage polarization was assessed as the ratio of M1-associated (*IL1b*, *MMP1b*, and *IL6*) to M2-associated (*IL10*, *IL4*, and *CD206)* gene expression. Human FLS (hFLS) isolated from synovial tissue of OA patients were treated with vehicle (DMSO) or HU308 following TNF-α or IL-1β stimulation to assess inhibition of catabolic/inflammatory gene expression.

Results: ACLR induces synovitis, progressively-worsening PTOA severity, and an immediate and sustained increase in both mechanical allodynia and knee hyperalgesia, which persist beyond the resolution of molecular inflammation. Enrichment of CB2, but not CB1, was observed in ACLR synovium at 3d, 14d, and 28d, and CB2 was found to be associated with F4/80 (+) cells, which are increased in number in ACLR synovium at all time points. The CB2 agonist HU308 strongly inhibited mBMDM M1-type polarization following stimulation with either IL-1β or conditioned medium from IL-1β-treated mFLS, which was characterized by reductions in *Il1b, Mmp1b*, and *Il6* and increases in *Cd206* gene expression. Cannabidiol similarly inhibited IL-1β-induced mBMDM M1 polarization via a reduction in *Il1b* and an increase in *Cd206* and *Il4* gene expression. Lastly, in OA hFLS, HU308 treatment inhibited IL-1β-induced *CCL2*, *MMP1*, *MMP3*, and *IL6* expression and further inhibited TNF-α-induced *CCL2*, *MMP1*, and *GMCSF* expression, demonstrating human OA-relevant anti-inflammatory effects by targeting CB2.

Conclusions: Joint injury perturbs the intra-articular ECS, characterized by an increase in synovial F4/80(+) cells, which express CB2, but not CB1. Targeting CB2 in murine macrophages and human FLS induced potent anti-inflammatory and anti-catabolic effects, which indicates that the CB2 receptor plays a key role in regulating inflammatory signaling in the two primary effector cells in the synovium. The intraarticular ECS is therefore a potential therapeutic target for blocking pathological inflammation in future disease-modifying PTOA treatments.

* Address correspondence and reprint requests to: T. Maerz, Department of Orthopaedic Surgery, University of Michigan, Biomedical Sciences Research Building, Room 2017, 109 Zina Pitcher Place, Ann Arbor, 48109, MI, USA. Tel.: 734-936-2566.
E-mail address: tmaerz@umich.edu (T. Maerz).

https://doi.org/10.1016/j.joca.2021.09.003
1063-4584/

Introduction

While the exact pathophysiology of osteoarthritis (OA) and post-traumatic osteoarthritis (PTOA) remain unclear, there is increasing evidence that inflammation is a key regulator of their pathogenesis[1]. In idiopathic OA, inflammation develops gradually, manifesting as painful inflammatory flares[2]. In animal models of PTOA, injury-induced synovitis is more severe than in age-related OA, persisting for months and never resolving[3]. This rapidly developing inflammation and activation of pathogenic signaling may be responsible for the greater severity and more rapid progression of PTOA relative to OA[4,5]. As there are no approved disease-modifying drugs for the treatment of OA or PTOA[6], a greater understanding of mechanisms underpinning pathological inflammatory signaling and their relationship to disease progression is required.

In the synovium, the fibroblast-like synoviocyte (FLS) and synovial macrophage act as primary effector cells orchestrating inflammation[7], yet their crosstalk is poorly understood in the context of PTOA. Cytokines such as TNF-α and IL-1β[3], chemokines such as CCL2[8] and proteolytic enzymes such as members of the MMP and ADAMTS family[9], are implicated in the pathogenic signaling underlying PTOA, and these factors are upregulated by fibroblast-like synoviocytes (FLS) and synovial macrophages following joint injury. As such, there is great interest in inhibiting these in order to protect articular cartilage from degeneration or to promote healing[10]. Unfortunately, anti-TNF-α and anti-IL-1β therapies have failed to show clinically significant benefits in endstage OA[11,12], while IL-1RA administration was shown to provide acute pain relief following ACL injury[13]. Traditional first-line therapies such as corticosteroids and NSAIDs provide transient relief with no impact on disease-driving processes[14,15]. Recently, the endocannabinoid system (ECS) has emerged as a target for treatment of arthritic pain and inflammation[16]. The ECS signals through two receptors: cannabinoid receptor type 1 (CB1), found primarily in the central nervous system (CNS) and cannabinoid receptor type 2 (CB2), found on immune cells[16]. The ECS is perturbed in clinical OA[17], evidenced by elevated expression of receptors and endocannabinoids in osteoarthritic but not healthy synovial fluid[17]. Previously, targeting CB2 was shown to exert anti-inflammatory effects in rheumatoid arthritis (RA) FLS[18,19]. Agonizing CB2 in peritoneal macrophages promoted an anti-inflammatory phenotype by decreasing ROS production[20] and attenuating proliferation of inflammatory M1 macrophages[21]. The phenotype of the macrophage following injury plays a vital role in the progression and resolution of inflammation. While recent studies have demonstrated that macrophages can exist in complex multidimensional phenotypic states[22,23], the M1-M2 spectrum is commonly used to describe pro-vs anti-inflammatory macrophages: pro-inflammatory M1-macrophages secrete cytokines and proteases which promote inflammation and tissue catabolism to clear damaged tissues. M2-macrophages work to resolve inflammation and promote tissue healing by expressing anti-inflammatory factors, and it is recognized that imbalance of macrophage phenotype results in increased catabolism and persistent inflammatory damage due to increased production of cartilage-degrading enzymes[24,25]. To date, it remains unknown whether targeting CB2 within the FLS or macrophage mitigates inflammation following joint injury.

Some previous studies have assessed the link between nociception and ECS signaling in central and peripheral pain[26]. Inhibition of fatty acid amide hydrolase and monoacyl glycerol lipase, enzymes responsible for endocannabinoid degradation[16], reduced pain in models of nerve injury[27], noxious pain[28], and inflammatory injury[29] by elevating endocannabinoids. In the context of arthritis, Malfait *et al.* demonstrated that the phytocannabinoid cannabidiol (CBD) lowered histological OA scores in inflammatory OA[30], and Philpott *et al.* showed that CBD reduced nociception in inflammatory arthritis[31], supporting the ECS as a treatment target in OA. However, less is known about ECS signaling in the context of joint injury and PTOA. Specifically, it remains unclear whether activation of the ECS coincides with the development of synovitis and nociceptive changes after injury. Distinct intra-articular tissues and cells that upregulate ECS receptors in response to joint trauma remain similarly uncharacterized. To that end, this study sought to demonstrate how joint injury perturbs the intra-articular ECS, assess how ECS perturbation coincides with the development of synovitis and PTOA after joint trauma, and characterize how CB2 mediates anti-inflammatory effects in FLS and macrophages. We employed a noninvasive, tibial compression-based model of ACL rupture, which recapitulates high-magnitude joint loading, traumatic tissue damage, and acute synovitis representative of human ACL injury. While tissue-level degenerative remodeling and some molecular alterations have been characterized using this model in both the mouse and rat[32–37], the longitudinal changes to nociception following noninvasive ACL rupture remain uncharacterized. Thus, a secondary objective was to characterize nociception and elucidate how pain coincides with local ECS perturbation in our noninvasive ACLR model.

Methods

Mice and noninvasive anterior cruciate ligament rupture model

With IACUC approval, 12-14 week-old male C57BL/6J mice were randomized to sham (anesthesia and analgesia only) or tibial compression-based, noninvasive ACL rupture (ACLR) using a random number generator. Within the ACLR group, mice were further randomized to study time point (3, 14, or 28 days). The ACLR protocol is modified from that by Christiansen *et al.*[32]. Mice were anesthetized with isofluorane and placed prone on a custom fixture on a materials testing system (Electroforce 3300AT, TA Instruments, New Castle, DE). The right knee was flexed to 100°, and the paw was mounted in 30° dorsiflexion. After preloading and preconditioning, a 1.5 mm displacement was rapidly applied to the paw (10 mm/s), causing tibial subluxation and ACL rupture. Mice were administered a single dose of subcutaneous carprofen (5 mg/kg), allowed *ad libitum* cage activity and access to food and water, and housed in ventilated cages of up to 5 mice (mix of Sham and ACLR) with a 12-h light/dark cycle. Mice were euthanized via CO2 asphyxia.

Assessment of mechanical allodynia and knee hyperalgesia

To evaluate central and local nociceptive alterations following injury, mechanical allodynia and knee hyperalgesia were assessed longitudinally at 1d, 3d, 7d, 14d, 21d, and 28d post-ACLR. Mechanical allodynia was assessed via Von Frey testing using Touch Test Sensory Evaluators (Stoelting Co, Wood Dale, IL). Withdrawal response was determined using an ascending response method[38]. Knee-specific hyperalgesia was quantified using a Randall–Selitto device (IITC Life Science, Woodland Hills, CA). The convex tip of the pressure applicator was applied to the medial knee joint until a vocal or physical response occurred. The average force of triplicate applications was calculated.

Cytokine and chemokine protein assays

To quantify cytokine and chemokine protein concentrations in the joint, the whole knee joint was removed by dislocating the distal femoral and proximal tibial physes, taking care not to disrupt

the joint capsule, freed of muscle, and homogenized in 1 mL of tissue lysis buffer using a tissue homogenizer (Precellys Evolution, Bertin Instruments, Rockville, MD). Following centrifugation to separate debris, protein concentrations were determined using a Multiplex ELISA (Luminex xMAP, Luminex Corp, Austin, TX) and the Milliplex MAP Mouse Cytokine/Chemokine Magnetic Bead Panel (MCYTOMAG-70K, Millipore-Sigma, Burlington, MA).

Histological analyses

At 3d, 14d, and 28d post-ACLR, whole hindlimbs were collected, fixed for 48 h in 10% neutral-buffered formalin, rinsed with water, and paraffin processed. Sagittal sections (5 μm) spanning the medial joint, spaced ~100 μm, were cut and stained with Safranin-O/Fast Green (SafO) and Hematoxylin & Eosin (H&E). Our analyses focused on the medial joint as greater disease severity develops in this compartment in the ACLR model[32]. Sections were imaged at 20x and qualitatively scored for PTOA[39] and synovitis severity[40] by three blinded observers using established grading schemes (Supplemental Tables 1 and 2). Scores were averaged across sections to obtain average scores for each rater and then averaged across raters to obtain aggregate scores for each limb.

For immunofluorescence, epitopes were retrieved using a pressure cooker for 6 min in a sodium citrate buffer, pH = 6.0. Medial joint sections were incubated overnight with primary antibody, stained with secondary antibody (Supplemental Table 3), and counterstained with Hoechst 33342 (Invitrogen, H3570, Carlsbad, CA). Slides were imaged at 20x (3 sections per limb) (Lionheart FX, Biotek, Winooski, VT). Tissue masks were manually contoured using ImageJ to isolate anterior and posterior synovial regions, and CellProfiler[41] was used to measure cell-associated F4/80, CB1, and CB2 signal. Cells were classified as either positive or negative using a *k*-means clustering algorithm (Matlab, The Mathworks, Nattick MA), with clusters set to 2 (positive/negative), as previously described[42]. Nuclear masks were further utilized to measure total cellularity and cellular density in synovium by quantifying the number of nuclei in each mask using CellProfiler (See Fig. S4).

Primary murine bone marrow-derived macrophage (mBMDM) isolation and culture

Whole bone marrow was isolated by centrifugation of femora and tibiae of uninjured C57BL6/J mice ($n = 5$ unique isolations) and incubated in DMEM containing 10% FBS and 20 ng/mL M-CSF (Gibco, PMC2044, Carlsbad, CA) for 7 days[43]. For each unique isolation, Murine bone marrow-derived macrophages (mBMDM)s were then plated in 12-well plates (200,000 cells/well) and pre-treated with media containing 1μM DMSO, the specific CB2 agonist HU308 (1μM) (Tocris, Bristol, UK, Cat. No 3088), or cannabidiol (10μM) (Cayman Chemical, Ann Arbor, MI, Item No. 90080) for 30 min. Media was replaced with fresh media containing PBS or 10 ng/mL IL-1β (R&D Systems, Minneapolis, MN, 401-ML), in addition to DMSO, 1μM HU308, or 10μM CBD[44,45]. After 8 h, cells were lysed with TRIzol and stored at −80°C until gene expression analysis. For experiments using mFLS conditioned media (CM), mFLS were isolated from adult injured C57Bl/6 mice ($n = 6$ unique isolations) (Supplemental Method 1), cultured until passage 4, and treated with PBS or 10 ng/mL IL-1β for 48 h (3 replicates per treatment). CM was collected, and equal volumes from each unique experiment were pooled for both PBS-treated (PBS-CM) and IL-1β-treated (IL-1β-CM) mFLS. mBMDM ($n = 3$ unique isolations) were plated as described above and incubated with either PBS-CM or IL-1β-CM, along with 1μM DMSO or 1μM HU308[44]. After 48 h, cells were lysed with TRIzol and stored at −80°C until gene expression analysis.

Immunocytochemistry

Primary mFLS or mBMDMs were plated on coverslips and fixed using 4% paraformaldehyde. Cells were permeabilized, blocked, incubated overnight in primary antibody solution, and incubated in secondary antibody solution (Supplemental Table 3). Nuclei were stained with Hoecht 33,342 and coverslips were imaged (Lionheart FX, Biotek, Winooskie, VT).

Primary human osteoarthritic FLS (hFLS) isolation and culture

Human FLS (hFLS) were generously donated by Dr. David Fox at the University of Michigan. With IRB approval (HUM00089350), human synovial biopsies were collected from 7 patients (4 male, 3 female) undergoing total knee arthroplasty (TKA) with the primary diagnosis of end-stage osteoarthritis. Tissues were minced and digested as described[46]. hFLS were cultured and stored in liquid nitrogen until experiments. hFLS were expanded, and following four passages, plated in triplicate at 150,000 cells per well, serum starved, and treated with DMEM containing PBS, 10 ng/mL IL-1β or 10 ng/mL TNF-α (R&D Systems, Minneapolis, MN, 410-MT) and treated with DMSO or 1 μM HU308 for 48 h. Cells were then lysed with TRIzol and stored at −80°C.

Gene expression analyses

RNA was isolated using chloroform extraction and converted to cDNA (High Capacity cDNA Reverse Transcription Kit, Applied Biosystems; California, USA), producing a final cDNA concentration of 10 ng/μL. RT-PCR was performed by mixing 10 ng cDNA with SYBR Green master mix (Applied Biosystems, MA, USA) and primers (Supplemental Table 4), and run using a Bio-Rad T100 Thermal-Cycler (Bio-Rad, Berkeley, CA). Gene expression data was normalized to the respective housekeeping gene (*Atpb5b* for mFLS and whole synovial tissue, *Gapdh* for mBMDM, and *Hprt1* for hFLS) using the 2^{-}-ΔCT method, and this value was further normalized to the expression of the contralateral limb (for tissue qPCR experiments) or the PBS/DMSO control groups (for cell-based experiments).

Statistical analyses

Statistical analyses were performed in SPSS (v27, IBM, Armonk, NY) and Prism 9.0 (Graphpad, San Diego, CA). Two-Way Repeated Measures ANOVA with Sidak post-hoc tests was used to assess differences in continuous outcomes within the ACLR group whenever both limbs were analyzed in separate groups of mice at different time points (limb as a within-subject factor and time point as a between-subject factor). Comparisons of continuous outcomes between either limb in the ACLR group to the single independent Sham group were performed using one-way ANOVA with Dunnett's post-hoc test (Sham as the control group). Three-Way Repeated Measures ANOVA with Sidak post-hoc tests was used to assess differences in continuous outcomes measured longitudinally on the same mice in the Sham and ACLR groups (limb and time point as within-subject factors and group as between-subject factor). Ordinal scoring outcomes or non-normally distributed continuous outcomes were compared between matched limbs within the ACLR group using Wilcoxon Signed Rank tests with Sidak family-wise *P* value correction. Ordinal scoring outcomes or non-normally distributed continuous outcomes were compared between independent time points within the ACLR group or between Sham and

ACLR using Kruskal–Wallis tests with Dunn's post-hoc tests. Two-Way Repeated Measures ANOVA with Sidak post-hoc tests was used to assess differences in continuous outcomes from *in vitro* experiments with matched treatments within unique cell isolations (cytokine stimulation and treatment group as within-subject factors). *P* values below 0.05 were considered significant. Numerical between-group differences from statistical analyses are tabulated in Appendix 1.

Results

ACL rupture induces acute synovitis that persists through the development of PTOA

Sham and contralateral (CL) limbs exhibited normal synovia; the synovial lining appeared 1 to 3 cells thick, with no subsynovial inflammatory infiltrate and no exudate present in the joint space.

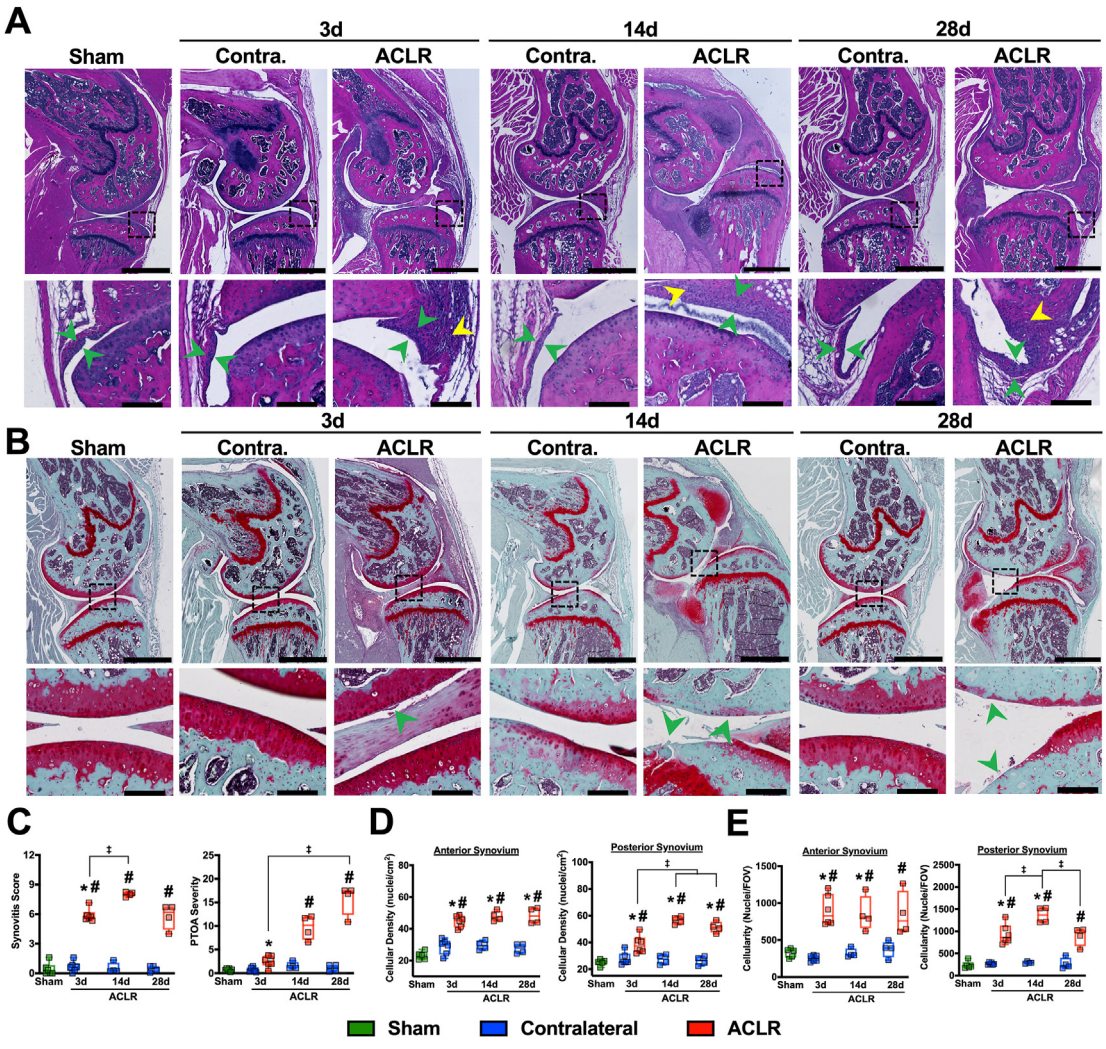

Fig. 1 OSTEOARTHRITIS PREVENTION Osteoarthritis and Cartilage

ACLR induces lingering synovitis concurrent with progressively-worsening PTOA. A) Representative H&E-stained sections of Sham, CL, and ACLR limbs, with emphasis on anterior synovium. Location of high-magnification views are denoted by dashed boxes. Green arrow heads denote synovial lining thickness, which increases in ACLR limbs, while yellow arrowheads denote inflammatory infiltrate, which was not observed in CL or Sham synovia. B) Representative SafO/Fast-Green stained sections of Sham, CL, and ACLR limbs. High-magnification views are denoted by dashed boxes and represent regions of maximal articular cartilage damage. Arrowheads denote cartilage erosion and damage, which progressively worsens and becomes more widespread following injury. A-B): Scale bar is 1,000 μm on whole-joint images and 100 μm for high-magnification views. C) Synovitis and PTOA severity scoring[39,40]. $n = 4–6$ mice per group/time point. * = $p < 0.05$ compared to CL within each time point; Wilcoxon Signed Rank Test. # = $p < 0.05$ compared to Sham; Kruskal–Wallis test with Dunn's post-hoc test (Sham as the control group). ‡ = $p < 0.05$ between time points within ACLR; Kruskal–Wallis test with Dunn's post-hoc test. D-E) Cellular density (D) and Total cellularity (E) determined using quantitative histomorphometry in anterior and posterior synovium. $n = 4–6$ mice per group/time point. * = $p < 0.05$ compared to CL within each time point, ‡ = $p < 0.05$ between time points within ACLR; Two-way repeated measures ANOVA with Sidak post-hoc test (limb as within-subject factor and time point as between-subject factor). # = $p < 0.05$ compared to Sham; one-way ANOVA with Dunnett's post-hoc test (Sham as the control group).

3d post-ACLR, synovia exhibited notable lining hyperplasia, early inflammatory infiltrate, and minor sublining fibrosis [Fig. 1(A)]. By 14d, synovitis reached maximal severity, with significant lining hyperplasia, marked fibrosis, large pockets of inflammatory infiltrate, and focal ectopic cartilage formation [Fig. 1(A)]. By 28d, synovitis resolved slightly, with reduced lining hyperplasia and inflammatory infiltrate but with notably persistent fibrosis. Synovial changes coincided with the progression of PTOA, with maximal synovitis severity observed at 14d as PTOA severity increased to 28d [Fig. 1(C)]. SafO staining demonstrated progressive cartilage erosion and proteoglycan loss up to 28d, most notably on the posterior tibial plateau and central femoral condyle [Fig. 1(B)]. Large, immature osteophytes formed by 14d, which partially mineralized by 28d. Histomorphometric analysis of synovia demonstrated 100–150% increases in cellular density and 150–200% increases in total cellularity compared to CL and Sham throughout the study [Fig. 1(D) and (E)]. The posterior synovium exhibited a slight reduction in both cellularity and density from 14d to 28d, while the anterior synovium did not exhibit this reduction of synovitis. Notably, subsidence in total synovial cellularity, but not cellular density, was noted at 28d relative to CL [Fig. 1(E)], indicative of gradual resolution of inflammation with lasting injury-induced remodeling.

Nociceptive sensitization occurs immediately after joint trauma and remains altered following resolution of molecular inflammation

To ascertain nociceptive alterations following ACLR, we longitudinally measured mechanical allodynia and knee hyperalgesia. ACLR mice exhibited an immediate and sustained increase in mechanical allodynia, noted by a 50–70% reduction in paw withdrawal threshold relative to Sham and CL from 1d to 28d [Fig. 2(A)]. Knee

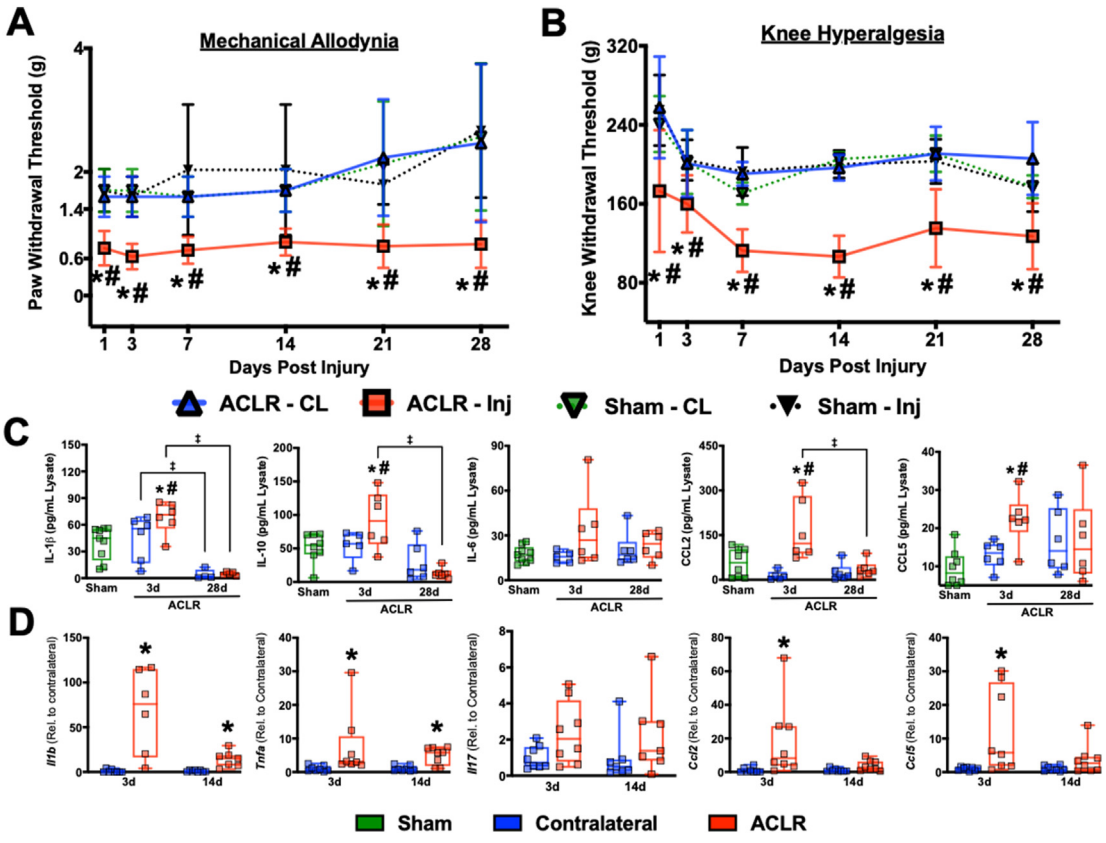

Fig. 2 OSTEOARTHRITIS PREVENTION Osteoarthritis and Cartilage

ACLR exacerbates mechanical allodynia and knee hyperalgesia. A) Mechanical allodynia measured via von Frey testing. B) Knee hyperalgesia measured via pressure application-based Randall–Selitto testing. A, B). $n = 6$ mice per group measured longitudinally. * = $p < 0.05$ compared to CL within each group; # $p < 0.05$ compared to Sham; Three-way repeated measures ANOVA (limb and time point as within-subject factors and group as between-subject factor) with Sidak post-hoc test. C) Cytokine and chemokine protein concentrations in whole knees following ACLR. $n = 5$–8 mice per group/time point. * = $p < 0.05$ compared to CL within each time point, ‡ = $p < 0.05$ between time points within ACLR; Two-way repeated measures ANOVA with Sidak post-hoc test (limb as within-subject factor and time point as between-subject factor). # = $p < 0.05$ compared to Sham; one-way ANOVA with Dunnett's post-hoc test (Sham as the control group). D) Expression of inflammatory genes by qPCR in whole synovial tissue from ACLR and contralateral joints. Relative expression was normalized to *Atpb5b* mRNA levels and the mean Contralateral value for each gene was set to 1. $n = 6$–8 mice per time point. * = $p < 0.05$ compared to CL within each time point; Wilcoxon Signed Rank Test.

hyperalgesia also developed immediately but slightly more progressively, with a ~20–25% reduction in threshold compared to Sham at 1d followed by a ~30–45% reduction compared to both Sham and CL from 3d to 28d [Fig. 2(B)]. To elucidate how molecular markers of inflammation coincide with observed nociceptive alterations, whole-joint homogenates were assayed for IL-1β, IL-6, IL-10, CCL2 and CCL5. At 3d, ACLR joints had a significant increase in IL-1β, IL-10, CCL2, and CCL5 compared to CL and sham [Fig. 2(C)]. Additionally, the levels of CCL5 in the contralateral limbs showed a slight but not statistically significant elevation relative to sham, indicating potential systemic inflammatory alterations following ACLR. By 28d, all protein markers returned to baseline [Fig. 2(C)]. To assess synovial involvement in molecular inflammation, whole synovial tissue was collected for gene expression analyses at early stages of disease (3d and 14d). Synovial *Il1b*, *Tnfa*, *Ccl2,* and *Ccl5* were significantly elevated at 3d, while *Il17a* nominally increased

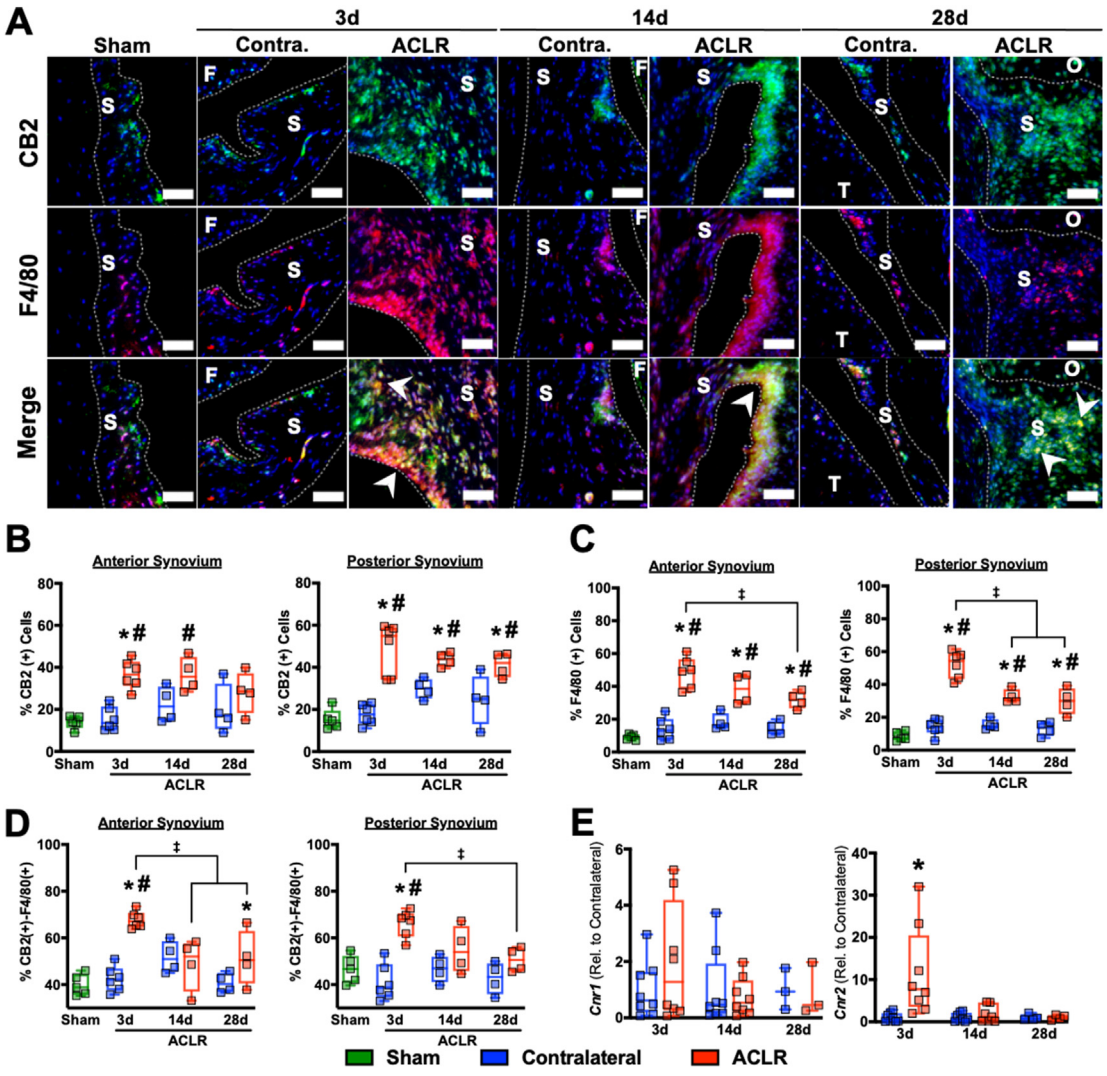

Fig. 3 OSTEOARTHRITIS PREVENTION Osteoarthritis and Cartilage

The CB2 receptor is upregulated by F4/80(+) synovial cells following ACL rupture. A) Immunofluorescent staining of cannabinoid receptor 2 and the monocyte/macrophage marker F4/80 in synovium. S = Synovium, F = Femur, T = Tibia, O = Osteophyte. Green: CB2, Red: F4/80, Blue: DAPI. Scale bar is 50 μm. Arrows denote regions of double positive cells (yellow signal), indicative of F4/80(+) cells expressing CB2 within injured synovium. B-D). Quantification of the proportion of CB2-positive cells (B), F4/80-positive cells (C), and CB2-positive cells which are also F4/80-positive (D) in synovium. $n = 4–6$ mice per group/time point. * = $p < 0.05$ compared to CL within each time point, ‡ = $p < 0.05$ between time points within ACLR; Two-way repeated measures ANOVA with Sidak post-hoc test (limb as within-subject factor and time point as between-subject factor). # = $p < 0.05$ compared to Sham; one-way ANOVA with Dunnett's post-hoc test (Sham as the control group). E) Gene expression of *CNR1* and *CNR2* by qPCR in whole synovial tissue from ACLR and contralateral joints. Relative expression was normalized to *Atpb5b* mRNA levels and the mean Contralateral value for each gene was set to 1. $n = 3–8$ mice per time point. * = $p < 0.05$ compared to CL within each time point. Wilcoxon Signed Rank Test.

[Fig. 2(D)]. By 14d, *Ccl2* and *Ccl5* had returned to the levels of CL, while *Il1b* and *Tnfa* remained elevated [Fig. 2(D)]. Taken together, these results demonstrate that noninvasive ACLR has an immediate effect on central and local nociception, which remain altered following resolution of molecular inflammation in the joint.

CB2 is acutely upregulated by F4/80(+) synovial cells following joint injury

We then sought to characterize how joint injury impacts intraarticular CB receptor expression. CB1 was sparsely expressed, with some expression in the synovial stroma but no ACLR-induced changes (Fig. S1). CB2 expression was also minimal throughout healthy synovia in Sham and CL, but abundant injury-induced expression was noted in both lining and sublining layers of ACLR synovia [Fig. 3(A)]. Quantitative analysis demonstrated a significant increase in CB2(+) synovial cells in anterior and posterior synovium compared to Sham and CL at 3d, with posterior synovium exhibiting a 30–60% increase at 14d and 20–80% increase at 28d. A return of CB2 to the level of CL was noted in anterior, but not posterior synovium, at 28d, indicating potential compartment-specific alterations to the CB2(+) cell populations following ACLR [Fig. 3(B)]. Histologic results were corroborated by synovial qPCR, demonstrating no injury-induced *Cnr1* changes but a significant upregulation of *Cnr2* at 3d relative to CL, followed by a recovery to baseline [Fig. 3(E)]. We hypothesized that cells of the monocyte/macrophage population were responsible for synovial CB2 upregulation. F4/80 counterstaining demonstrated significant enrichment of F4/80(+) cells following injury within the posterior and anterior synovium, with maximal injury-induced increases at 3d and gradually decreasing up to day 28 [Fig. 3(C)]. Approximately half of all CB2(+) cells were F4/80(+), and joint injury increases this proportion: at 3d, both anterior and posterior synovia had significantly higher percentages of CB2(+) F4/80(+) cells compared to Sham and CL, with an average of 67.7± 3.6% and 66.1± 5.7%, respectively [Fig. 3(D)], and the proportion of these double positive cells was maximum at 3d, which began to reduce as inflammation resolved at later time points. Immunofluorescence indicates that this overlap is consistent in lining and sub-lining layers, and double-positive signal in the lining demonstrates distinct palisades of cells, indicative of synovial lining macrophages. Taken together, these results indicate that F4/80(+) cells are enriched in the synovium and upregulate CB2 following joint injury.

CB2 agonism and cannabidiol mitigate pro-inflammatory polarization of macrophages

Following our observation of F4/80(+) cells enriching in the synovium and expressing CB2 after joint injury, we set out to assess whether targeting CB2 can exert anti-inflammatory effects in macrophages. Given the absence of an established synovial macrophage isolation protocol, we employed the widely-utilized BMDM model. We found that mBMDM robustly express *Cnr2* [Fig. 4(A)], corroborated by ICC of CB2 [Fig. 4(B)], with no alteration from cannabinoid or IL-1β treatment. We sought to determine whether CB2 agonism alters the macrophage polarization response to IL-1β, given that M1-type macrophage polarization plays a disease-promoting role in OA[25]. We calculated a macrophage polarization score, based on Paige *et al.*[47], as the ratio of M1-associated (*IL1b*, *MMP1b*, and *IL6*) to M2-associated (*IL10*, *IL4*, and *CD206)* gene expression. Treatment with the CB2 agonist HU308 strongly inhibited IL-1β-induced M1 polarization (Control: 17.05 ± 3.69, HU308: 3.00 ± 1.2) [Fig. 4(C)]. This inhibition was driven by significant reductions in *Il1b* and *Mmp1b* and an increase in *Cd206* [Fig. 4(C)]. As a pharmacological experiment, we also treated mBMDM with CBD, which elicited similar inhibitory effects on macrophage M1 polarization, driven by a significant reduction in *Il1b* and increases in *Cd206* and *Il4* expression [Fig. 4(C)].

Although we did not test whether CB2 is expressed by FLS *in vivo*, we measured *Cnr2* gene expression and CB2 protein in primary mFLS isolated from healthy and 7d ACLR knee joints (Supplemental Method 1). We found little to no detectable CB2 protein or *Cnr2* transcript expressed by mFLS *in vitro*, with similar expression levels between cells from healthy and 7d ACLR joints, and neither IL-1β nor TNF-α upregulated *Cnr2* expression (Fig. S2). As the crosstalk between FLS and macrophages orchestrates pathological inflammation in arthritis, we sought to assess whether FLS can polarize macrophages *in vitro* and whether CB2 agonism mediates this polarization. CM was generated from mFLS treated for 48 h with PBS (PBS-CM) or 10 ng/mL IL-1β (IL-1β-CM) (equally pooled across six unique isolations). IL-1β-CM strongly polarized mBMDM towards an M1 phenotype, and this was significantly abrogated by CB2 agonism (Control: 9.02 ± 0.94, HU308: 2.75 ± 0.86) [Fig. 4(D)]. This reduction in polarization was driven by significant decreases in *Il1b* and *Il6*, and a nominal increase in *Cd206* [Fig. 4(D)]. Furthermore, unstimulated mBMDM (i.e., PBS-CM-treated) exhibited a significant decrease in *Il6* and increase in *Il4* expression due to HU308 treatment [Fig. 4(D)], demonstrating anti-inflammatory effects by CB2 agonism even in the absence of inflammatory stimulus. Collectively, these results demonstrate that targeting the ECS via both direct CB2 agonism and pharmacologically using CBD inhibits M1 macrophage polarization *in vitro*.

CB2 agonism inhibits IL-1β- and TNF-α-induced inflammatory and catabolic gene expression in human OA FLS

As a further translational assessment of the anti-inflammatory effects of targeting CB2, we cultured hFLS from synovial biopsies obtained during TKA for end-stage OA. Although we did not find notable *Cnr2* expression by murine FLS, we sought to assess whether human FLS from end-stage OA express CB receptors and whether CB2 agonism elicits similar anti-inflammatory properties as observed in mBMDMs. Our results show that human OA FLS expressed *CNR2* at low but detectable levels, and neither IL-1β or TNF-α treatment changed *CNR2* expression (Fig. S3). CB2 agonism significantly inhibited IL-1β-induced upregulation of *CCL2*, *MMP1*, *MMP3*, and *IL6* [Fig. 5(A)] and also inhibited TNF-α-induced upregulation of *CCL2*, *MMP1*, and *GMCSF* [Fig. 5(B)]. Our sample of seven patients exhibited variable responses, with obvious responders and non-responders to HU308, but we did not observe any significant correlations between *CNR2* expression levels and HU308-induced treatment effects (data not shown). Collectively, these data demonstrate that targeting CB2 in hFLS from endstage OA blocks cytokine-induced inflammatory and catabolic genes expression.

Discussion

Although the ECS is implicated in inflammation and nociception, little is known about its role in PTOA. Using a noninvasive model of ACL rupture in mice, we found that CB2, but not CB1, is strongly induced in the synovium acutely after joint trauma and that expression is confined to F4/80(+) cells, indicative of synovial macrophages. *In vitro*, we found that both direct CB2 agonism and CBD treatment markedly inhibit macrophage M1 polarization, and CB2 agonism also induced anti-inflammatory and anti-catabolic effects in human OA FLS.

Our findings demonstrate that perturbation of the intra-articular ECS following joint trauma is characterized by an expansion of CB2(+) F4/80(+) cells in the synovium, indicative of synovial macrophages infiltrating and proliferating in response to injury and

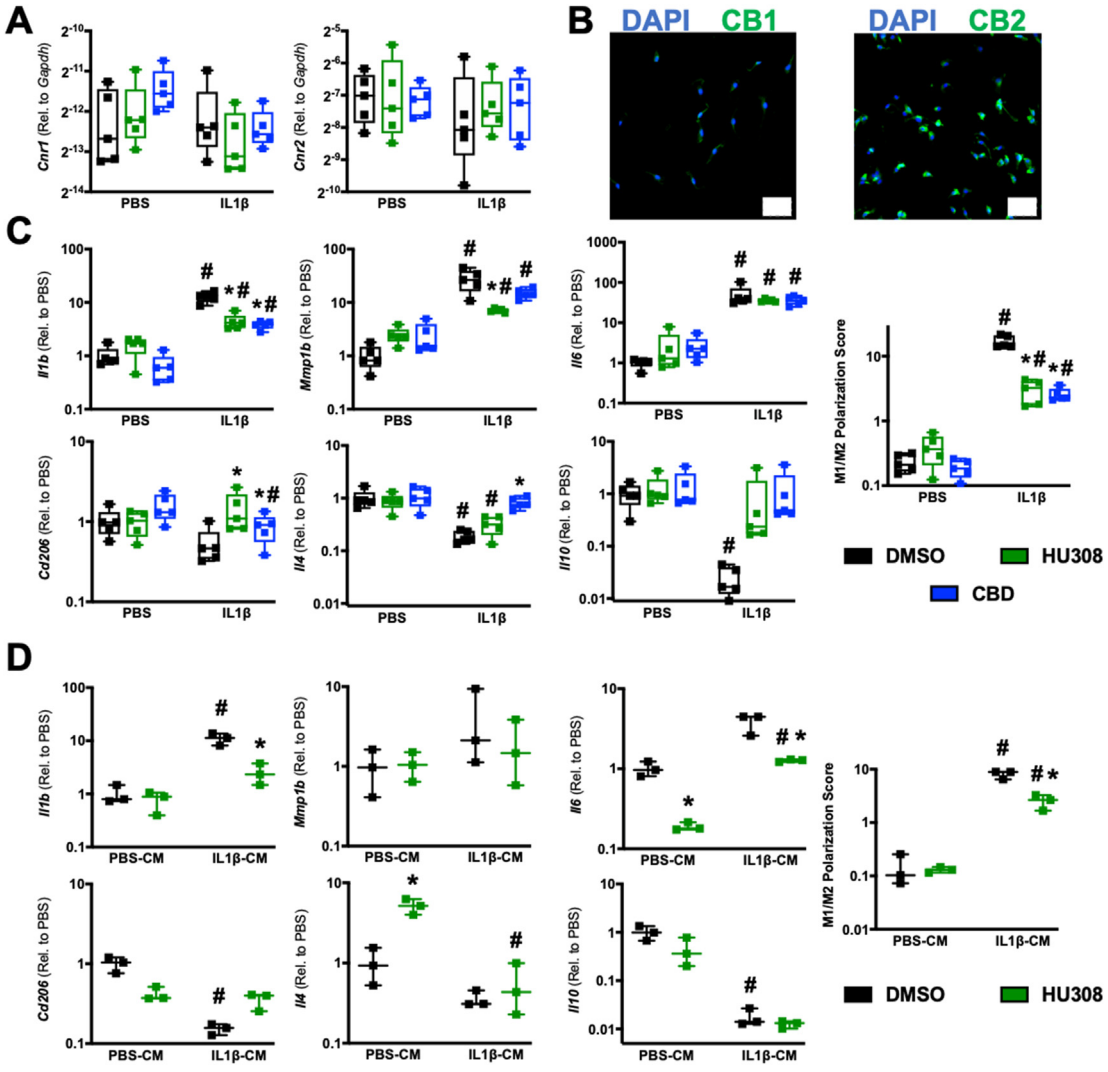

Fig. 4 OSTEOARTHRITIS PREVENTION Osteoarthritis and Cartilage

mBMDM express CB2 and exhibit anti-inflammatory responses to CB2 agonist and Cannabidiol treatment. A) Macrophage expression of ***Cnr1*** and ***Cnr2*** is not altered by IL-1β or cannabinoid treatment. $n = 5$ unique isolations/cultures. B) Immunocytochemistry of cultured mBMDM demonstrates widespread CB2 protein expression, with little to no CB1. Scale bar is 50 μm. C) M1-and M2-associated gene expression and composite M1/M2 polarization score of mBMDM stimulated with PBS or IL-1β and treated with DMSO, the CB2 agonist HU308, or CBD. Relative expression was normalized to *Gapdh* mRNA levels, and the mean DMSO-treated PBS value for each gene was set to 1. $n = 5$ unique isolations/cultures. * = $p < 0.05$ compared to respective DMSO within PBS or within IL1β group; # = $p < 0.05$ compared to respective PBS group within DMSO, HU308, or CBD treatment. Two-way repeated measures ANOVA with Sidak post-hoc test. D) M1-and M2-associated gene expression and composite M1/M2 polarization score of mBMDM stimulated with conditioned media (CM) from PBS-treated or IL-1β-treated FLS and further treated with DMSO or HU308. Relative expression was normalized to *Gapdh* mRNA levels, and the mean DMSO-treated PBS-CM value for each gene was set to 1. $n = 3$ unique isolations/cultures. * = $p < 0.05$ compared to respective DMSO within PBS-CM or within IL1β-CM group; # = $p < 0.05$ compared to respective PBS-CM group within DMSO or HU308 treatment. Two-way repeated measures ANOVA with Sidak post-hoc test.

upregulating CB2. Significant increases in the proportion of CB2(+) cells were measured in both anterior and posterior synovial compartments 3 days post-ACLR. This increase corresponded with a densification of F4/80(+) cells, and the proportion of CB2(+) cells that were also F4/80(+) was acutely elevated relative to controls. Macrophages are a critical component in the inflammatory response in PTOA, and M1 macrophages are linked to pain and tissue degeneration in osteoarthritis[25]. However, the presence of M1 macrophages is not always indicative of active inflammation, and the presence of M2 macrophages is not definitively indicative of tissue healing. Indeed, both ends of the polarization spectrum are required for tissue homeostasis, and joint injury causes a long-term imbalance of macrophage phenotype, tilted towards the M1 state, which further perpetuates tissue damage[25]. Macrophages of

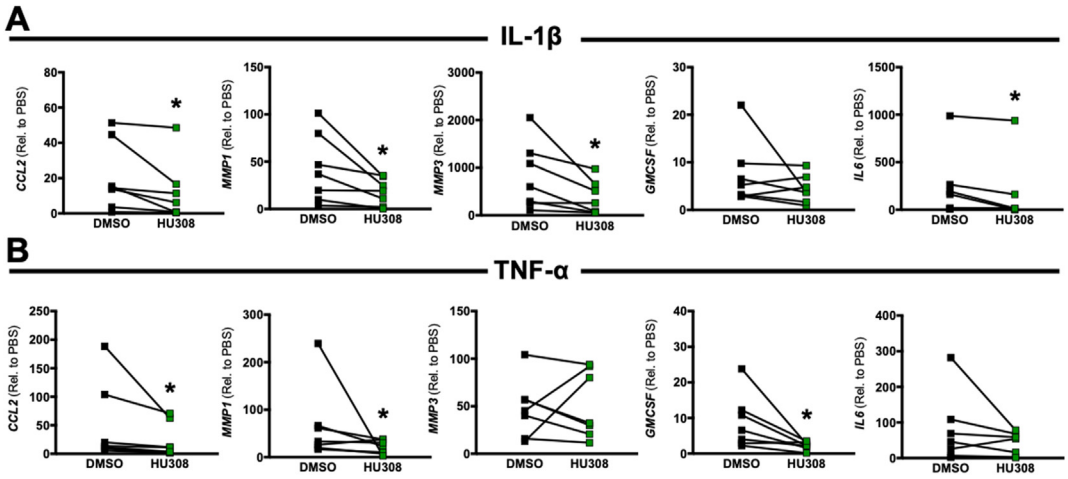

Fig. 5 OSTEOARTHRITIS PREVENTION Osteoarthritis and Cartilage

CB2 agonist treatment induces anti-inflammatory effects in cytokine-treated human OA FLS. Inflammatory and catabolic gene expression following stimulation with 10 ng/mL IL-1β (A) or 10 ng/mL TNF-α (B) and treatment with either DMSO or the CB2 agonist HU308. $n = 7$ unique isolations/cultures from human synovial biopsies (* = $p < 0.05$, Wilcoxon Signed Rank Test.).

various types express CB2[48,49], and our data indicates that synovial macrophages upregulate CB2 in response to injury, making them a potential therapeutic target for blocking injury-induced inflammation. Direct CB2 agonism in RA previously modulated macrophage phenotype, reducing disease severity[50]. Furthermore, CB2 agonism in surgical OA mitigated disease severity, while global deletion of CB2 increased severity and susceptibility to spontaneously develop OA[51]. Tomar *et al.* showed that CB2 agonism *in vitro* increased IL-10 production in M1 macrophages, and increased expression of M2 markers in M2 macrophages, while suppressing the *in vivo* expression of M1 markers and increasing expression of M2 markers in acute liver failure[52]. Our work extends this evidence, demonstrating that CB2 agonism strongly mitigates *in vitro* M1 mBMDM polarization following treatment with IL-1β. Using an OA-relevant panel of M1 and M2 genes, we demonstrated that CB2-mediated inhibition of the M1-phenotype is driven by reduced expression of *Il1b* and *Mmp1b*, with increased expression of *Cd206*. To further demonstrate the translatability of cannabinoids, we showed that cannabidiol can similarly mitigate *in vitro* M1 polarization induced by IL-1β, driven by reductions in *Il1b* and increased *Cd206* and *Il4*. Of note, CBD was particularly potent in blocking IL-1β-induced reduction in *Il4*, and CBD treatment recovered *Il4* expression of IL-1β-treated cells to the levels of PBS-treated cells. Lastly, we showed that CM from FLS treated with IL-1β induces M1-like macrophage polarization, which is strongly inhibited by CB2 agonism. These findings provide key evidence of the ability of CB2 agonism to inhibit the pro-inflammatory crosstalk between FLS and macrophages.

Our results demonstrate that the human OA FLS express *CNR2*, and are responsive to CB2 agonism, while mFLS from both healthy and 7d ACLR joints express *Cnr2* at negligible levels. Human synovial biopsies were obtained from end-stage OA patients, whereas murine samples were obtained from healthy or acutely-injured joints. We propose that both species-specific and disease chronicity-specific effects govern these differences. Previous research in tendinopathy has shown that chronic inflammation may reprogram fibroblasts to exhibit hypersensitivity to inflammatory agonism[53], and further studies are required to ascertain whether chronic disease processes alter the synovial fibroblast population to express CB2 in later-stage PTOA and whether inflammation-related mechanisms govern this induction. Thus, future studies should assess CB2 agonism in hFLS isolated from patients following ACL injury as a more representative comparison to our murine studies.

To the authors' knowledge, this is the first report of nociceptive alterations after noninvasive ACLR in mice. ACLR causes an immediate increase in mechanical allodynia, with a 50–70% reduction in paw withdrawal threshold maintained for the duration of study. Knee-specific hyperalgesia also developed immediately but slightly more progressively, with a 30–45% reduction in withdrawal threshold noted from 3d to 28d. Of note, we found that nociception remained altered even beyond the resolution of molecular inflammation. Our results indicate a more rapid onset of nociceptive changes compared to the murine DMM model, which exhibits significant alterations to knee hyperalgesia from 14d post-surgery onward[54]. Collectively, this demonstrates model-specific nociceptive changes, and the mechanisms underlying these changes following joint injury remain unclear. CCL2 has been implicated in driving OA pain by promoting the infiltration of inflammatory monocytes[8]. In DMM-induced OA, ablation of CCL2 suppressed inflammatory markers, reduced inflammatory cell infiltration, and reduced pain sensitization[8,55]. Recently, inhibition of CCL2-CCR2 signaling via both genetic ablation and pharmacological antagonism of CCR2 alleviated established hyperalgesia in DMM-induced OA[56]. We observed CCL2 protein and gene expression increases acutely after injury, and given the concurrent F4/80(+) cell proliferation, the role of CCL2 in orchestrating inflammation and nociceptive alterations after ACLR requires further study. Future work also should characterize the influx/enrichment of nociceptive neurons after joint trauma to identify which specific intra-articular tissues promote pain in PTOA.

This study is not without limitations. In whole-joint protein analyses, the exact tissue(s) contributing to inflammatory protein

production are unknown and require further analysis. Our qPCR analyses only used contralateral controls and no sham samples; systemic inflammation may be elevated following ACLR, which could impact contralateral gene expression. This study utilized only male mice but given reports of differential OA/PTOA severity between male and female C57BL/6J mice[57], further studies are needed to understand whether injury-induced inflammation and ECS perturbation are sex-specific in this model. Given the synovial focus of this study, we did not comprehensively assess CB1 and CB2 in other joint tissues such as cartilage, menisci, and subchondral bone. Our analysis of F4/80(+) cells within the synovium leads us to conclude that enrichment of CB2 is due to macrophage proliferation; however, F4/80 is also expressed by immature monocytes, neutrophils, and dendritic cells, and the exact identity of CB2+ F4/80+ cells in the synovium requires further study. While we assessed CNR1 and CNR2 gene expression in hFLS, CB1 and CB2 immunostaining of human synovial biopsies would serve to confirm presence/absence of these receptors at the protein level. Lastly, our study does not assess later-stage disease in mice, potentially missing inflammation- and ECS-related changes specific to end-stage disease.

To conclude, ACLR leads to lingering synovitis that persists through the resolution of molecular inflammation while inducing both central and peripheral sensitization. Acutely, CB2 is enriched in the joint and is strongly associated with F4/80(+) synovial cells, which greatly increase in number following joint injury. Targeting CB2 in mBMDM and hFLS potently inhibits cytokine-induced upregulation of catabolic and proinflammatory genes. Thus, the intra-articular ECS represents a druggable target for inducing anti-inflammatory effects, and future work is needed to understand how phytocannabinoids such as CBD may target the ECS as a disease-modifying PTOA treatment.

Author contributions

PMR, CJR, SR, AK, and TM contributed to the conception and design of the studies. PMR, CJR, LL, LJ, SG, RB, SR, AK, and ME contributed to the acquisition of data. PMR, CJR, LJ, SR, AK, and TM contributed to data analysis. PMR and TM drafted the article and revised it critically for important intellectual content. All authors approved of the final version for submission. TM takes responsibility for the work as a whole.

Conflict of interest

No authors have financial disclosures relevant to the study.

Funding sources

This study was funded in part by a Research Advisory Committee pilot grant from the Department of Orthopaedic Surgery at the University of Michigan. PMR was funded by NIH T32 Grant (5T32AR007080-40). AJK was supported by a Michigan Pioneer Postdoctoral Fellowship from the University of Michigan. Histology and imaging work was supported by the Michigan Integrative Musculoskeletal Health Core Center (P30 AR069620, National Institute of Arthritis and Musculoskeletal and Skin Diseases). Multiplex protein analyses were supported by the Michigan Diabetes Research Center (P30 DK020572, National Institute of Diabetes and Digestive and Kidney Diseases).

Acknowledgements

The authors would like to acknowledge Dr. Daniel Clauw, Dr. Kurt Hankenson, Dr. Gus Rosania, and Dr. David Fox for their mentorship and guidance in designing and executing experiments. The authors would like to thank Dr. Steven Harte for the use of the von Frey filaments and Dr. Giancarlo Vanini for the use of the handheld algesiometer. The authors would also like to acknowledge Phillip Campbell for his expertise with culturing hFLS.

Supplementary data

Supplementary data to this article can be found online at https://doi.org/10.1016/j.joca.2021.09.003.

References

1. Scanzello CR. Role of low-grade inflammation in osteoarthritis. Curr Opin Rheumatol 2017;29(1):79–85.
2. Greene MA, Loeser RF. Aging-related inflammation in osteoarthritis. Osteoarthritis Cartilage 2015;23(11):1966–71.
3. Lieberthal J, Sambamurthy N, Scanzello CR. Inflammation in joint injury and post-traumatic osteoarthritis. Osteoarthritis Cartilage 2015;23(11):1825–34.
4. Thomas NP, Wu WJ, Fleming BC, Wei F, Chen Q, Wei L. Synovial inflammation plays a greater role in post-traumatic osteoarthritis compared to idiopathic osteoarthritis in the Hartley Guinea pig knee. BMC Muscoskel Disord 2017;18(1):556.
5. Buckwalter JA. Articular cartilage: injuries and potential for healing. J Orthop Sports Phys Ther 1998;28(4):192–202.
6. Karsdal MA, Michaelis M, Ladel C, Siebuhr AS, Bihlet AR, Andersen JR, *et al.* Disease-modifying treatments for osteoarthritis (DMOADs) of the knee and hip: lessons learned from failures and opportunities for the future. Osteoarthritis Cartilage 2016;24(12):2013–21.
7. Tu J, Hong W, Zhang P, Wang X, Körner H, Wei W. Ontology and function of fibroblast-like and macrophage-like synoviocytes: how do they talk to each other and can they Be targeted for rheumatoid arthritis therapy? Front Immunol 2018;9:1467.
8. Miotla Zarebska J, Chanalaris A, Driscoll C, Burleigh A, Miller RE, Malfait AM, *et al.* CCL2 and CCR2 regulate pain-related behaviour and early gene expression in post-traumatic murine osteoarthritis but contribute little to chondropathy. Osteoarthritis Cartilage 2017;25(3):406–12.
9. Haslauer CM, Elsaid KA, Fleming BC, Proffen BL, Johnson VM, Murray MM. Loss of extracellular matrix from articular cartilage is mediated by the synovium and ligament after anterior cruciate ligament injury. Osteoarthritis Cartilage 2013;21(12):1950–7.
10. Ghouri A, Conaghan PG. Update on novel pharmacological therapies for osteoarthritis. Ther Adv Musculoskelet Dis 2019;11. 1759720x19864492.
11. Chevalier X, Goupille P, Beaulieu AD, Burch FX, Bensen WG, Conrozier T, *et al.* Intraarticular injection of anakinra in osteoarthritis of the knee: a multicenter, randomized, double-blind, placebo-controlled study. Arthritis Rheum 2009;61(3):344–52.
12. Cohen SB, Proudman S, Kivitz AJ, Burch FX, Donohue JP, Burstein D, *et al.* A randomized, double-blind study of AMG 108 (a fully human monoclonal antibody to IL-1R1) in patients with osteoarthritis of the knee. Arthritis Res Ther 2011;13(4):R125.
13. Kraus VB, Birmingham J, Stabler TV, Feng S, Taylor DC, Moorman 3rd CT, *et al.* Effects of intraarticular IL1-Ra for acute anterior cruciate ligament knee injury: a randomized controlled pilot trial (NCT00332254). Osteoarthritis Cartilage 2012;20(4):271–8.
14. Marcum ZA, Hanlon JT. Recognizing the risks of chronic nonsteroidal anti-inflammatory drug use in older adults. Ann Long Term Care 2010;18(9):24–7.

15. Wernecke C, Braun HJ, Dragoo JL. The effect of intra-articular corticosteroids on articular cartilage: a systematic review. Orthop J Sports Med 2015;3(5). 2325967115581163.
16. Carmen LP, A BS, Roger N, Rafael M. Involvement of the endocannabinoid system in osteoarthritis pain. Eur J Neurosci 2014;39(3):485–500.
17. Richardson D, Pearson RG, Kurian N, Latif ML, Garle MJ, Barrett DA, *et al*. Characterisation of the cannabinoid receptor system in synovial tissue and fluid in patients with osteoarthritis and rheumatoid arthritis. Arthritis Res Ther 2008;10(2):R43.
18. Lowin T, Pongratz G, Straub RH. The synthetic cannabinoid WIN55,212-2 mesylate decreases the production of inflammatory mediators in rheumatoid arthritis synovial fibroblasts by activating CB2, TRPV1, TRPA1 and yet unidentified receptor targets. J Inflamm 2016;13:15.
19. Fechtner S, Singh AK, Srivastava I, Szlenk CT, Muench TR, Natesan S, *et al*. Cannabinoid receptor 2 agonist JWH-015 inhibits interleukin-1β-induced inflammation in rheumatoid arthritis synovial fibroblasts and in adjuvant induced arthritis rat via glucocorticoid receptor. Front Immunol 2019;10(1027).
20. Han KH, Lim S, Ryu J, Lee C-W, Kim Y, Kang J-H, *et al*. CB1 and CB2 cannabinoid receptors differentially regulate the production of reactive oxygen species by macrophages. Cardiovasc Res 2009;84(3):378–86.
21. Braun M, Khan ZT, Khan MB, Kumar M, Ward A, Achyut BR, *et al*. Selective activation of cannabinoid receptor-2 reduces neuroinflammation after traumatic brain injury via alternative macrophage polarization. Brain Behav Immun 2018;68:224–37.
22. Culemann S, Grüneboom A, Nicolás-Ávila J, Weidner D, Lämmle KF, Rothe T, *et al*. Locally renewing resident synovial macrophages provide a protective barrier for the joint. Nature 2019;572(7771):670–5.
23. Harasymowicz NS, Rashidi N, Savadipour A, Wu CL, Tang R, Bramley J, *et al*. Single-cell RNA sequencing reveals the induction of novel myeloid and myeloid-associated cell populations in visceral fat with long-term obesity. Faseb J 2021;35(3), e21417.
24. Chen Y, Jiang W, Yong H, He M, Yang Y, Deng Z, *et al*. Macrophages in osteoarthritis: pathophysiology and therapeutics. Am J Transl Res 2020;12(1):261–8.
25. Wu CL, Harasymowicz NS, Klimak MA, Collins KH, Guilak F. The role of macrophages in osteoarthritis and cartilage repair. Osteoarthritis Cartilage 2020;28(5):544–54.
26. Russo EB. Clinical endocannabinoid deficiency reconsidered: current research supports the theory in migraine, fibromyalgia, irritable bowel, and other treatment-resistant syndromes. Cannabis Cannabinoid Res 2016;1(1):154–65.
27. Kamimura R, Hossain MZ, Unno S, Ando H, Masuda Y, Takahashi K, *et al*. Inhibition of 2-arachydonoylgycerol degradation attenuates orofacial neuropathic pain in trigeminal nerve-injured mice. J Oral Sci 2018;60(1):37–44.
28. Jee Kim M, Tanioka M, Woo Um S, Hong SK, Hwan Lee B. Analgesic effects of FAAH inhibitor in the insular cortex of nerve-injured rats. Mol Pain 2018;14. 1744806918814345.
29. Ahn K, Johnson DS, Mileni M, Beidler D, Long JZ, McKinney MK, *et al*. Discovery and characterization of a highly selective FAAH inhibitor that reduces inflammatory pain. Chem Biol 2009;16(4):411–20.
30. Malfait AM, Gallily R, Sumariwalla PF, Malik AS, Andreakos E, Mechoulam R, *et al*. The nonpsychoactive cannabis constituent cannabidiol is an oral anti-arthritic therapeutic in murine collagen-induced arthritis. Proc Natl Acad Sci U S A 2000;97(17):9561–6.
31. Philpott HT, O'Brien M, McDougall JJ. Attenuation of early phase inflammation by cannabidiol prevents pain and nerve damage in rat osteoarthritis. Pain 2017;158(12):2442–51.
32. Christiansen BA, Anderson MJ, Lee CA, Williams JC, Yik JH, Haudenschild DR. Musculoskeletal changes following non-invasive knee injury using a novel mouse model of post-traumatic osteoarthritis. Osteoarthritis Cartilage 2012;20(7):773–82.
33. Chang JC, Sebastian A, Murugesh DK, Hatsell S, Economides AN, Christiansen BA, *et al*. Global molecular changes in a tibial compression induced ACL rupture model of post-traumatic osteoarthritis. J Orthop Res 2017;35(3):474–85.
34. Mendez ME, Sebastian A, Murugesh DK, Hum NR, McCool JL, Hsia AW, *et al*. LPS-Induced inflammation prior to injury exacerbates the development of post-traumatic osteoarthritis in mice. J Bone Miner Res 2020;35(11):2229–41.
35. Sebastian A, Murugesh DK, Mendez ME, Hum NR, Rios-Arce ND, McCool JL, *et al*. Global gene expression analysis identifies age-related differences in knee joint transcriptome during the development of post-traumatic osteoarthritis in mice. Int J Mol Sci 2020;21(1):364.
36. Maerz T, Kurdziel M, Newton MD, Altman P, Anderson K, Matthew HW, *et al*. Subchondral and epiphyseal bone remodeling following surgical transection and noninvasive rupture of the anterior cruciate ligament as models of post-traumatic osteoarthritis. Osteoarthritis Cartilage 2016;24(4):698–708.
37. Maerz T, Fleischer M, Newton MD, Davidson A, Salisbury M, Altman P, *et al*. Acute mobilization and migration of bone marrow-derived stem cells following anterior cruciate ligament rupture. Osteoarthritis Cartilage 2017;25(8):1335–44.
38. Deuis JR, Dvorakova LS, Vetter I. Methods used to evaluate pain behaviors in rodents. Front Mol Neurosci 2017;10:284.
39. Little CB, Barai A, Burkhardt D, Smith SM, Fosang AJ, Werb Z, *et al*. Matrix metalloproteinase 13-deficient mice are resistant to osteoarthritic cartilage erosion but not chondrocyte hypertrophy or osteophyte development. Arthritis Rheum 2009;60(12):3723–33.
40. Jackson MT, Moradi B, Zaki S, Smith MM, McCracken S, Smith SM, *et al*. Depletion of protease-activated receptor 2 but not protease-activated receptor 1 may confer protection against osteoarthritis in mice through extracartilaginous mechanisms. Arthritis & Rheumatology 2014;66(12):3337–48.
41. Lamprecht MR, Sabatini DM, Carpenter AE. CellProfiler: free, versatile software for automated biological image analysis. Biotechniques 2007;42(1):71–5.
42. Rzeczycki P, Woldemichael T, Willmer A, Murashov MD, Baik J, Keswani R, *et al*. An expandable mechanopharmaceutical device (1): measuring the cargo capacity of macrophages in a living organism. Pharm Res (N Y) 2018;36(1):12.
43. Francke A, Herold J, Weinert S, Strasser RH, Braun-Dullaeus RC. Generation of mature murine monocytes from heterogeneous bone marrow and description of their properties. J Histochem Cytochem 2011;59(9):813–25.
44. Gui H, Liu X, Wang ZW, He DY, Su DF, Dai SM. Expression of cannabinoid receptor 2 and its inhibitory effects on synovial fibroblasts in rheumatoid arthritis. Rheumatology (Oxford) 2014;53(5):802–9.
45. Coffey RG, Yamamoto Y, Snella E, Pross S. Tetrahydrocannabinol inhibition of macrophage nitric oxide production. Biochem Pharmacol 1996;52(5):743–51.
46. Kato H, Endres J, Fox DA. The roles of IFN-γ versus IL-17 in pathogenic effects of human Th17 cells on synovial fibroblasts. Mod Rheumatol 2013;23(6):1140–50.

47. Paige JT, Kremer M, Landry J, Hatfield SA, Wathieu D, Brug A, *et al.* Modulation of inflammation in wounds of diabetic patients treated with porcine urinary bladder matrix. Regen Med 2019;14(4):269–77.
48. Graham ES, Angel CE, Schwarcz LE, Dunbar PR, Glass M. Detailed characterisation of CB2 receptor protein expression in peripheral blood immune cells from healthy human volunteers using flow cytometry. Int J Immunopathol Pharmacol 2010;23(1):25–34.
49. Carlisle SJ, Marciano-Cabral F, Staab A, Ludwick C, Cabral GA. Differential expression of the CB2 cannabinoid receptor by rodent macrophages and macrophage-like cells in relation to cell activation. Int Immunopharm 2002;2(1):69–82.
50. Zhu M, Yu B, Bai J, Wang X, Guo X, Liu Y, *et al.* Cannabinoid receptor 2 agonist prevents local and systemic inflammatory bone destruction in rheumatoid arthritis. J Bone Miner Res 2019;34(4):739–51.
51. Sophocleous A, Borjesson AE, Salter DM, Ralston SH. The type 2 cannabinoid receptor regulates susceptibility to osteoarthritis in mice. Osteoarthritis Cartilage 2015;23(9):1586–94.
52. Tomar S, Zumbrun EE, Nagarkatti M, Nagarkatti PS. Protective role of cannabinoid receptor 2 activation in galactosamine/lipopolysaccharide-induced acute liver failure through regulation of macrophage polarization and microRNAs. J Pharmacol Exp Therapeut 2015;353(2):369–79.
53. Dakin SG, Buckley CD, Al-Mossawi MH, Hedley R, Martinez FO, Wheway K, *et al.* Persistent stromal fibroblast activation is present in chronic tendinopathy. Arthritis Res Ther 2017;19(1):16.
54. Miller RE, Ishihara S, Bhattacharyya B, Delaney A, Menichella DM, Miller RJ, *et al.* Chemogenetic inhibition of pain neurons in a mouse model of osteoarthritis. Arthritis Rheum 2017;69(7):1429–39.
55. Nees TA, Rosshirt N, Zhang JA, Reiner T, Sorbi R, Tripel E, *et al.* Synovial cytokines significantly correlate with osteoarthritis-related knee pain and disability: inflammatory mediators of potential clinical relevance. J Clin Med 2019;8(9).
56. Ishihara S, Obeidat AM, Wokosin DL, Ren D, Miller RJ, Malfait A-M, *et al.* The role of intra-articular neuronal CCR2 receptors in knee joint pain associated with experimental osteoarthritis in mice. Arthritis Res Ther 2021;23(1):1–12.
57. Ma HL, Blanchet TJ, Peluso D, Hopkins B, Morris EA, Glasson SS. Osteoarthritis severity is sex dependent in a surgical mouse model. Osteoarthritis Cartilage 2007;15(6):695–700.